water

MDPI

Communication

Analysis of $^{15}N\text{-}NO_3^-$ Via Anoxic Slurries Coupled to MIMS Analysis: An Application to Estimate Nitrification by Burrowing Macrofauna

Paula Carpintero Moraes [1], Diana Marcela Arroyave Gòmez [2], Fabio Vincenzi [3], Giuseppe Castaldelli [3], Elisa Anna Fano [3], Marco Bartoli [1,4,*] and Sara Benelli [1]

1 Department of Chemistry, Life Sciences and Environmental Sustainability, University of Parma, 43124 Parma, Italy; paula_cmoraes@yahoo.com (P.C.M.); sara.benelli@unipr.it (S.B.)
2 Facultad de Minas, OCEANICOS, Universidad Nacional de Colombia, 050036 Medellín, Colombia; dmarroya@unal.edu.co
3 Department of Life Sciences and Biotechnology, University of Ferrara, 44121 Ferrara, Italy; vncfba@unife.it (F.V.); ctg@unife.it (G.C.); fne@unife.it (E.A.F.)
4 Marine Science and Technology Center, University of Klaipeda, 92294 Klaipeda, Lithuania
* Correspondence: marco.bartoli@unipr.it; Tel.: +39-0521-905048

Received: 19 September 2019; Accepted: 1 November 2019; Published: 4 November 2019

Abstract: The increasing use of the stable isotope $^{15}N\text{-}NO_3^-$ for the quantification of ecological processes requires analytical approaches able to distinguish between labelled and unlabeled N forms. We present a method coupling anoxic sediment slurries and membrane inlet mass spectrometry to quantify dissolved $^{15}N\text{-}NO_3^-$ and $^{14}N\text{-}NO_3^-$. The approach is based on the microbial reduction of $^{14}N\text{-}NO_3^-$ and $^{15}N\text{-}NO_3^-$ mixed pool, the determination of the produced $^{29}N_2$ and $^{30}N_2$, and the calculation of the original $^{15}N\text{-}NO_3^-$ and $^{14}N\text{-}NO_3^-$ concentrations. The reduction is carried out in 12 mL exetainers containing 2 mL of sediment and 10 mL of water, under anoxia. To validate this approach, we prepared multiple standard solutions containing $^{15}N\text{-}NO_3^-$ alone or in combinations with $^{14}N\text{-}NO_3^-$, with final concentrations varying from 0.5 to 3000 µM. We recovered nearly 90% of the initial $^{14}N\text{-}NO_3^-$ or $^{15}N\text{-}NO_3^-$, over a wide range of concentrations and isotope ratios in the standards. We applied this method to a $^{15}N\text{-}NO_3^-$ dilution experiment targeting the measurement of nitrification in sediments with and without the burrower *Sparganophilus tamesis*. The oligochaete did not stimulate nitrification, likely due to limited ventilation and unfavorable conditions for nitrifiers growth. The proposed method is reliable, fast, and could be applied to multiple ecological studies.

Keywords: $^{15}N\text{-}NO_3^-$; slurry; denitrification; MIMS; nitrification; *Sparganophilus tamesis*

1. Introduction

Nitrogen (N) pollution and increasing eutrophication of aquatic environments have increased attention concerning the regulation of the N cycle by microbial and primary producer communities [1]. Different methods and techniques have been developed for measuring N transformations, in particular in sediments, and they are more and more based on the use of the N stable isotope ^{15}N [2–4]. Since the introduction of the isotope pairing technique (IPT) [5], denitrification has been a target process for nearly 25 years, and its role in aquatic ecosystems has been often overemphasized as compared to other microbial transformations [6]. The IPT is based on the addition of $^{15}N\text{-}NO_3^-$ to the water phase of micro or mesocosms and the quantification of the produced $^{29}N_2$ and $^{30}N_2$. The IPT should not be used when anammox contributes significantly to the N_2 production. Thus, a bioassay for anammox determination should be always performed before using this technique. Denitrification bioassays, besides the accurate determination of N_2 production within sediments, may be used to

determine $^{15}N\text{-}NO_3^-$ concentrations in the water phase, allowing experimental evaluations of other processes [7]. $^{15}N\text{-}NO_3^-$ determination, in combination with $^{15}N\text{-}NH_4^+$ analysis, may allow the precise quantification of relevant processes of the N cycle as the dissimilative reduction of nitrate to ammonium (DNRA) or the nitrification rate [8–10]. The latter are much less studied processes as compared to denitrification [6]. In recent years, the determination of N isotopes in dissolved N_2 has become fast and accurate thanks to the introduction of membrane inlet mass spectrometry (MIMS, [11]). The membrane inlet mass spectrometer does not require creating a headspace in water samples, which are circulated in a gas-permeable capillary where the dissolved gases are extracted by a vacuum and directed to the mass spectrometer [8,9,11].

Previous methodological reports for the determination of N isotopes in pools of $^{14}N\text{-}NO_3^-$ and $^{15}N\text{-}NO_3^-$ were based on bioassays with pure bacterial culture of denitrifiers, the quantification of $^{29}N_2$ and $^{30}N_2$ and of the ^{14}N to ^{15}N ratios [7,8]. Alternatively, $^{15}N\text{-}NO_3^-$ can be accurately determined via the use of strong reductants as cadmium and sodium azide, as the chemical reduction to N_2O and the analysis of the $^{14/15}N$ pool in the N_2O [12–14]. In this work, we propose a relatively simple, inexpensive and quick method to measure a wide range of concentrations of $^{14}N\text{-}NO_3^-$ and $^{15}N\text{-}NO_3^-$ combining anoxic sediment slurries and MIMS analysis. Original $^{14}N\text{-}NO_3^-$ and $^{15}N\text{-}NO_3^-$ concentrations are back calculated according to the equations and assumptions of the isotope pairing technique. We present here results from multiple laboratory tests aiming at the precise calibration of the method and of the specific performances of the sediment we employed (e.g., denitrification capacity, co-occurrence of anammox) under different experimental conditions (e.g., slurry concentrations, incubation time, variable isotopic ratios). The accurate determination of labelled and unlabeled dissolved nitrate has multiple implications in ecological studies of N cycling. In particular, it may offer the possibility to accurately assess the rates of nitrification in intact sediment cores, a process that is understudied as compared to other microbial N transformations. We therefore applied the method to a laboratory experiment targeting the rates of nitrification, calculated via the dilution of $^{15}N\text{-}NO_3^-$, in riverine sediments with and without the burrowing oligochaete *Sparganophilus tamesis*. Macrofauna, in order to promote aerobic conditions in their burrows and get rid of metabolic waste, pump oxic water within otherwise anoxic and ammonium-rich mud. The activity of bioturbating macrofauna can stimulate microbial nitrification and increase the production of $^{14}N\text{-}NO_3^-$ from the pore water $^{14}N\text{-}NH_4^+$ pool. Such production leads to decreasing $^{15}N\text{-}NO_3^-$ to $^{14}N\text{-}NO_3^-$ ratios in the water column, which are proportional to nitrification rates and can be accurately quantified.

2. Materials and Methods

Instead of using pure cultures of denitrifying bacteria or performing chemical reductions, we added eutrophic riverine sediments, which were collected from a shallow-water (50 cm) wetland area of the Mincio River (Northern Italy), to water samples containing labelled and unlabeled nitrate. Previous experiments suggested that these organic sediments display high rates of denitrification, whereas anammox was never detected [15]. Sediments were muddy, with an average porosity of 0.77 and an organic matter content of 9.2% as loss on ignition. They were collected via plexiglass liners; the upper 5 cm layer was extruded and sieved (0.5 mm sieve) to remove macrofauna and large debris and homogenized. Variable volumes of the sediment homogenate (from 0.5 to 6 mL, see the next paragraphs), together with glass beads, were transferred to 12 mL gas-tight vials with screw cap and rubber septum (Labco Exetainers, Lampeter, UK). The vials were then completely filled with water containing different concentrations of $^{15}N\text{-}NO_3^-$ ($K^{15}NO_3$ 98% atom, Cambridge Isotope Laboratories, MA, USA), previously flushed with pure N_2 to remove O_2. All treatments were done in triplicates and always combined with blanks (O_2-free deionized water). Once closed without bubbles, the exetainers were put on a rotating shaker in order to maintain sediments in suspension. They were incubated in the dark and at environment temperature (20 °C); the biological activity was stopped by the addition of $ZnCl_2$ (200 µL, 7 M). Thereafter, they were centrifuged, maintained at 4 °C and analyzed within two

weeks for $^{29}N_2$ and $^{30}N_2$ by MIMS (Bay Instruments, Easton, MD, USA) at the University of Ferrara (Ferrara, Italy).

With the purpose of experimentally defining the optimal slurry concentration and incubation time and to evaluate the efficiency of the method in terms of ^{15}N recovery along $^{15}N\text{-}NO_3^-$ concentrations series or variable ^{15}N to ^{14}N ratios in the dissolved nitrate pool, we performed four sequential tests, described in paragraphs 2.1 to 2.4 and summarized in Table 1.

Table 1. Summary of the experimental conditions of each test. Every tested condition was run in triplicate.

		$[^{15}N\text{-}NO_3^-]$ μM			$[^{14}N\text{-}NO_3^-]$ μM			Time (h)		[Slurries] mL L^{-1}		
Slurry concentration series		50			0			20		42 83 125 167	208 250 292 333	375 417 458 500
Time series		2 20 200 300			0			0.5 1 1.5 2 2.5 3	5 7 10 22 34 48	167		
Concentration series		0.5 2.5 5 10 20 30 40 50	75 100 150 200 300 400 500 600	700 800 900 1000 1500 2000 3000	0			20		167		
Quantification of labelled and unlabeled $N\text{-}NO_3^-$	(a)	0.2 0.6 2.5 6.5 16.5	33.0 50.0 67.0 83.5 93.5	97.5 99.4 99.8	99.8 99.4 97.5 93.5 83.5	67.0 50.0 33.0 16.5 6.5	2.5 0.6 0.2	20		167		
	(b)	37.5 40 42.5 45 47.5	50 52.5 55 57.5 60	62.5	62.5 60 57.5 55 52.5	50 47.5 45 42.5 40	37.5					

2.1. Slurry Concentration Series

In order to choose the appropriate sediment to water ratio of the slurry, we tested different slurry concentrations (from 42 to 500 mL L^{-1}, in triplicate), while we maintained a fixed level of $^{15}N\text{-}NO_3^-$ (50 μM). To this purpose, 12 different sediment to water ratios were analyzed (Table 1). All vials were incubated in the dark for 24 h.

2.2. Time Series Experiment

In order to determine the appropriate incubation time to denitrify the dissolved nitrate, we performed a time series experiment. To this purpose, slurries were realized using four different concentrations of $^{15}N\text{-}NO_3^-$ (from 2 to 1000 μM, in triplicate) that were incubated from 0.5 to 48 h (Table 1). The concentration of the slurry was fixed at 167 mL L^{-1} (2 mL of sediment and 10 mL of water). At different time intervals, for a total of 13 different incubation times, 3 exetainers per level of $^{15}N\text{-}NO_3^-$ were sacrificed, adding $ZnCl_2$ (200 μL, 7 M) to stop microbial activity.

2.3. Concentration Series Experiment

To quantify the total denitrification capacity of the microbial community in the sediment homogenate, a series of experiments were realized with increasing concentrations of $^{15}N\text{-}NO_3^-$. To this purpose, we tested 24 different levels of nitrate (from 0 to 3000 µM $^{15}N\text{-}NO_3^-$, in triplicate; Table 1). The concentration of the slurry was fixed at 167 mL L^{-1} and based on previous findings the vials were incubated in the dark for 20 h.

2.4. Quantification of Labelled and Unlabeled N-NO_3^-

As in most experimental applications, both labelled and unlabeled nitrate are present in solution, 24 standards containing different ratios of $^{14}N\text{-}NO_3^-$ and $^{15}N\text{-}NO_3^-$ (from 0.2 to 99.8 atom% of the isotope) were prepared in triplicate (Table 1). Regardless of the ratios of the two isotopes, the final nitrate concentration was always 100 µM. The concentration of the slurry was fixed at 167 mL L^{-1}, and the vials were incubated in the dark for 20 h.

2.5. Anammox Assay

In order to exclude the occurrence of anammox, which would introduce an error in the IPT calculations [16], we checked whether the production of $^{29}N_2$ followed the trend expected by the binomial distribution of $^{28}N_2$, $^{29}N_2$ and $^{30}N_2$ due to denitrification alone. To this purpose, we made a series of slurries (in triplicate) with variable $^{15}N\text{-}NO_3^-$ concentrations (from 5 to 200 µM) and a fixed $^{14}N\text{-}NO_3^-$ concentrations (50 µM). The occurrence of anammox would result in additional $^{29}N_2$ production from the combination of $^{14}NH_4^+$ and $^{15}N\text{-}NO_2^-$.

2.6. Calculations

The concentration of the total unlabeled N_2 (TN_2) present in the samples was calculated from the $^{28}N_2$ signal of the MIMS. The concentrations of $^{29}N_2$ and $^{30}N_2$ (µM) were calculated from Equations (1) and (2):

$$\left[^{29}N_2\right] = \frac{^{29}N_2}{^{28}N_2} \times \left[TN_2\right], \quad (1)$$

$$\left[^{30}N_2\right] = \frac{^{30}N_2}{^{28}N_2} \times \left[TN_2\right]. \quad (2)$$

where $^{29}N_2/^{28}N_2$ and $^{30}N_2/^{28}N_2$ are the excess of $^{29}N_2$ and $^{30}N_2$ over the total $^{28}N_2$, measured as mass 29 and 30 to 28 ratios. The excess was calculated correcting measured ratios by the natural background values.

The concentration of the $^{28}N_2$ originated via denitrification of $^{14}N\text{-}NO_3^-$ was calculated from the Equation (3), assuming a binomial distribution of the produced $^{28}N_2$, $^{29}N_2$ and $^{30}N_2$ [5]:

$$\left[^{28}N_2\right] = \frac{\left(\frac{\left[^{29}N_2\right]}{2}\right)^2}{\left[^{30}N_2\right]} \quad (3)$$

The concentrations of $^{15}N\text{-}NO_3^-$ and $^{14}N\text{-}NO_3^-$ (µM) were then calculated with Equations (4) and (5):

$$\left[^{14}N - NO_3^-\right] = \left[^{29}N_2\right] + 2 \times \left[^{28}N_2\right], \quad (4)$$

$$\left[^{15}N - NO_3^-\right] = \left[^{29}N_2\right] + 2 \times \left[^{30}N_2\right]. \quad (5)$$

2.7. Application of the Method to a $^{15}N\text{-}NO_3^-$ Dilution Experiment to Measure Nitrification Rates in Bioturbated Sediments

2.7.1. Microcosm Set Up and Incubation

We applied the proposed method in order to quantify the rates of nitrification in bare and bioturbated sediments (Figures 1 and 2). Nitrification can be assumed as the sum of the nitrate produced within sediments and diffusing to the water column ($^{14}N\text{-}NO_3^-$-efflux) and of the nitrate produced within sediments, diffusing to the anoxic layers and denitrified (D_N). Nitrate efflux can be calculated by means of dilution of $^{15}N\text{-}NO_3^-$ in the water phase [17], while coupled nitrification–denitrification can be calculated by applying the IPT [5]. The calculations proposed here would lead to underestimated nitrification activity in the presence of significant NO_3^- uptake by primary producers at the sediment–water interface or of high rates of DNRA.

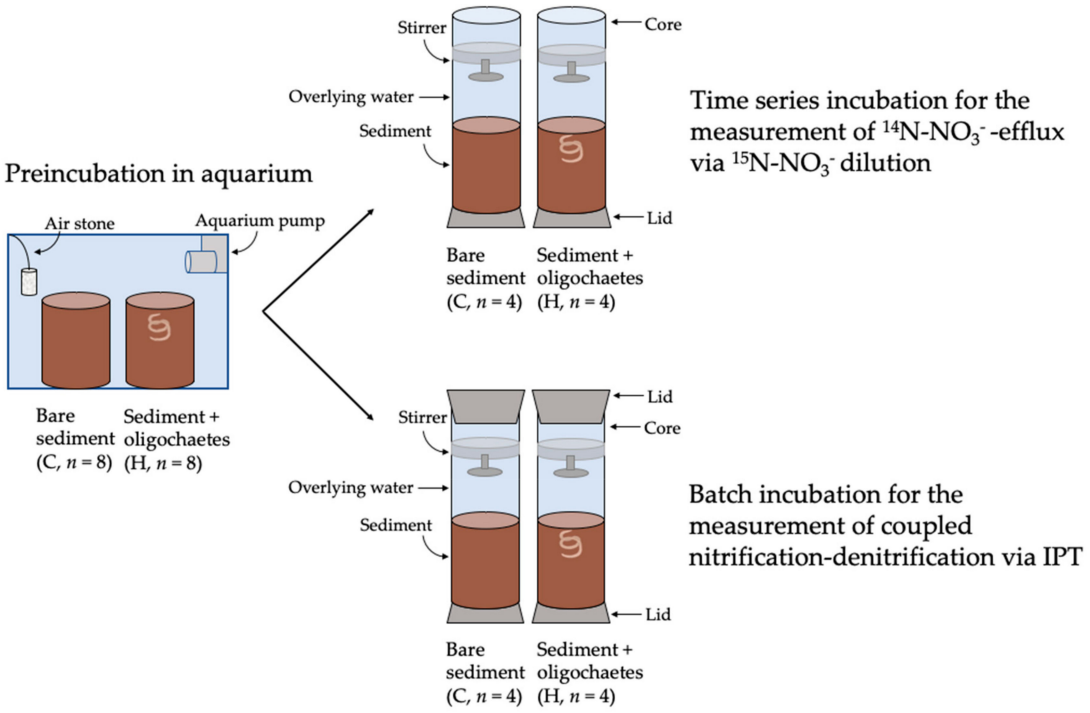

Figure 1. A scheme of the experimental design that consisted of two treatments: bare sediment (C, n = 8) and sediment with oligochaetes (H, n = 8). After one week of preincubation in the aquarium, microcosms were separated into two groups in order to measure $^{14}N\text{-}NO_3^-$-efflux (Section 2.7.2) and coupled nitrification-denitrification (Section 2.7.3).

In order to measure nitrification rates in bioturbated sediment, nearly 5 L of sediment was collected from the same area previously described and sieved to remove large debris and macrofauna, then homogenized. The sediment homogenate was transferred into cylindrical plexiglass microcosms (n = 16, inner diameter 8 cm, height 10 cm) as described in [18]. After one day of acclimatization, individuals of the oligochaete *S. tamesis* were added in 8 microcosms to a final density of 800 ind m^{-2} (high density treatment H), reflecting in situ values [19]. All oligochaetes burrowed within a few minutes into the sediments. The remaining 8 microcosms, without macrofauna, were used as controls (C). Microcosms C and H were preincubated for one week in large aquaria containing well mixed and aerated in situ water (NH_4^+ 1.8 ± 0.2 µM, NO_3^- 103.7 ± 3.6 µM; NO_2^- 3.1 ± 0.1 µM) maintained at 20 °C. After the preincubation, 8 microcosms (4 with bare sediments and 4 with oligochaetes) were included in liners with a water phase of 16 cm, mixed by Teflon-coated stirring bars rotating at 60 rpm and with the top open, in order to ensure oxic conditions (Figure 1). Each liner was added with 1.8 mL of 15 mM $^{15}N\text{-}NO_3^-$ solution to have a final concentration of nearly 30 µM $^{15}N\text{-}NO_3^-$ (and an enrichment of

nearly 30%, the $^{14}N\text{-}NO_3^-$ concentration being nearly 100 µM). Shortly after the addition of the labelled nitrate solution (t0) and after 2.5, 5, 7.5 and 10 h of dark incubation (t1, t2, t3, t4, respectively), water samples (12 mL) were collected from each liner, filtered, and immediately frozen for later analysis. From a water phase of 800 mL in each microcosm, a total of 12 mL × 5 samplings = 60 mL (<8% of the water volume) were collected during the course of the experiment. All water samples were then treated as previously described in order to quantify $^{14}N\text{-}NO_3^-$ and $^{15}N\text{-}NO_3^-$ concentrations.

2.7.2. Calculation of $^{14}N\text{-}NO_3^-$-Efflux from Sediments

The total flux of $^{14}N\text{-}NO_3^-$ out of the sediment ($^{14}N\text{-}NO_3^-$-efflux) was calculated with two methods. The first (A) is based on linear regressions applied to the concentration changes of $^{14}N\text{-}NO_3^-$ and $^{15}N\text{-}NO_3^-$ during the course of the experiment, as detailed in the graphical representation of Figure 2, while the second (B) is based on the equation proposed by [17].

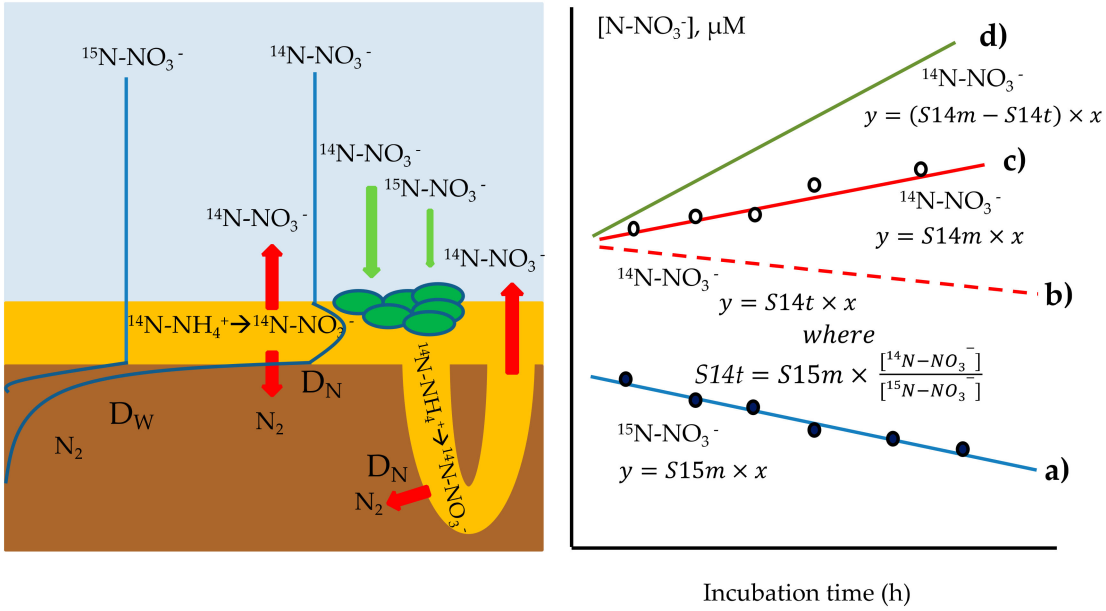

Figure 2. Graphical representation of the calculation of the efflux of nitrate from the sediment to the water column due to nitrification ($^{14}N\text{-}NO_3^-$-efflux). The theoretical uptake of $^{14}N\text{-}NO_3^-$ (**b**) is calculated from measured $^{15}N\text{-}NO_3^-$ consumption (**a**). The nitrate efflux (**d**) is calculated subtracting the theoretical nitrate uptake (**b**) from that measured experimentally (**c**). Dots are experimental data. See the text for more details.

Method A

The slope of the regression between measured $^{15}N\text{-}NO_3^-$ concentration and time (S15m) integrates all $^{15}N\text{-}NO_3^-$ consuming processes (i.e., uptake, denitrification, DNRA) (Figure 2). Knowing the ratio between $^{15}N\text{-}NO_3^-$ and $^{14}N\text{-}NO_3^-$ concentrations in the water column at t0 and the slope S15m, the analogous theoretical slope S14t, integrating all the $^{14}N\text{-}NO_3^-$ consuming processes, can be calculated (S14t = S15m × [$^{14}N\text{-}NO_3^-$/$^{15}N\text{-}NO_3^-$]). If significant, the difference between S14t and the slope of measured $^{14}N\text{-}NO_3^-$ trend (DS14 = S14m − S14t) represents the $^{14}N\text{-}NO_3^-$-efflux (Figure 2). The latter in fact is sustained by nitrification of $^{14}N\text{-}NH_4^+$ within sediments, occurring also for the small sedimentary pool of $^{15}N\text{-}NH_4^+$ (0.366, which is the natural abundance of ^{15}N in the ammonium pool). The $^{14}N\text{-}NO_3^-$-efflux (µmol N m^{-2} h^{-1}) is then calculated according to Equation (6):

$$\left[{}^{14}N - NO_{3\ \text{efflux}}^{-}\right] = (\text{S14m} - \text{S14t}) \times 10 \times \text{h}, \quad (6)$$

where *S14m* and *S14t* (μmol N $L^{-1}h^{-1}$) are the measured and theoretical slopes of the regression between unlabeled nitrate concentration and time, *h* is the height of the water phase (cm), and *10* is a unit conversion factor.

Method B

According to [17], the $^{14}N\text{-}NO_3^-$-efflux (μmol N m^{-2} h^{-1}) is calculated with Equation (7):

$$\left[{}^{14}N - NO^-_{3\ efflux}\right] = \left(\frac{Ci \times (f - i)}{0.366\ - f}\right) \times 10 \times \frac{h}{t}, \quad (7)$$

where Ci is the initial concentration of $^{15}N\text{-}NO_3^-$ (μM, t0), f and i are the final (t4) and initial (t0) fractions of $^{15}N\text{-}NO_3^-$ in the total $^{14+15}N\text{-}NO_3^-$ pool, respectively, 0.366 is the natural abundance of ^{15}N in the ammonium pool, h (cm) is the height of the water phase, and *t* (h) is the incubation time.

2.7.3. Measurement of Coupled Nitrification–Denitrification

The remaining eight microcosms were incorporated into liners and the isotope pairing technique was applied [5,20]. Briefly, $^{15}N\text{-}NO_3^-$ was added to the water phase to a final concentration of 30 μM, as in previous experiments. Shortly after the addition, a subsample (12 mL) was collected in order to analyze the $^{15}N\text{-}NO_3^-$ to $^{14}N\text{-}NO_3^-$ ratio in the water phase, as previously explained. Then, the cores were immediately closed at the top with a rubber stopper and incubated in the dark for 4 h. At the end of the incubation, all cores were gently slurred and a subsample of the slurry collected, transferred into exetainers, and poisoned with 200 μL of $ZnCl_2$ 7 M. $^{29}N_2$ and $^{30}N_2$ produced via denitrification were analyzed by MIMS and calculations performed according to the assumptions and equations reported by [5]. It was then possible to calculate total denitrification and the contribution of the denitrification of nitrate diffusing to anoxic sediments from the water column (D_W) and the denitrification of nitrate produced within sediments via nitrification (D_N). We considered the IPT a reliable method as the anaerobic oxidation of ammonium to molecular nitrogen is generally not detected in eutrophic freshwater sediments [21]. However, we excluded the occurrence of anammox from the Mincio River sediments with a specific assay (see Section 3.5).

2.8. Statistical Analyses

In the nitrification experiment, the values of total $N\text{-}NO_3^-$-efflux were tested for normality using the Kolmogorov–Smirnov test. As the assumptions for normality were met, two-way analysis of variance (ANOVA) was employed to test for differences between the rates measured in the two treatments and between the methods utilized for the calculations.

3. Results and Discussion

3.1. Slurry Concentration Series

In the range from 42 to 500 mL of sediment per liter of slurry (from 0.5 to 6 mL in a final volume of 12 mL), the recovery of the added $^{15}N\text{-}NO_3^-$ (50 μM) was the same and averaged 89% (data not shown). This confirms previous findings that the enzymatic capacity of the denitrifier community is very large in the sediments we used [15]. When relatively low $^{15}N\text{-}NO_3^-$ concentrations are expected, a very small sediment volume can be added to the water samples to perform quantitatively the reduction to N_2. We standardized the method fixing the slurry concentration at 167 mL L^{-1} (2 mL of sediment and 10 mL of water sample) as most of our study areas, within the Po River Plain, may display very high NO_3^- concentrations, up to 1000 μM [22].

3.2. Time Series Experiment

The concentration of $^{15}N\text{-}NO_3^-$ calculated from the production of $^{30}N_2$ during the course of the time series experiment is reported in Figure 3. Concentrations of $^{15}N\text{-}NO_3^-$ (nearly 2, 20, 200 and 1000 μM) in the slurries at t0 are estimated, as they were not rigorously checked by spectrophotometric analyses. Nitrate reduction and the accumulation of labelled gas reached a plateau in <5 h when the $^{15}N\text{-}NO_3^-$ concentrations in the slurries were 2, 20, and 200 μM, while it took longer (nearly 20 h) at 1000 μM (Figure 3). The plateau was set at the concentration of $^{15}N\text{-}NO_3^-$ (± 5%) recovered after 48 h of slurry incubation and the appropriate incubation time was set graphically. During the anoxic incubation, we found trace amounts of $^{29}N_2$, due to microbial reduction of $^{14}N\text{-}NO_3^-$ in the $K^{15}NO_3$ salt used for this experiment (98% ^{15}N). Based on the results of this experiment, we set the incubation time of the following experiments at 20 h to optimize production of N_2 regardless of the initial concentration of $^{15}N\text{-}NO_3^-$.

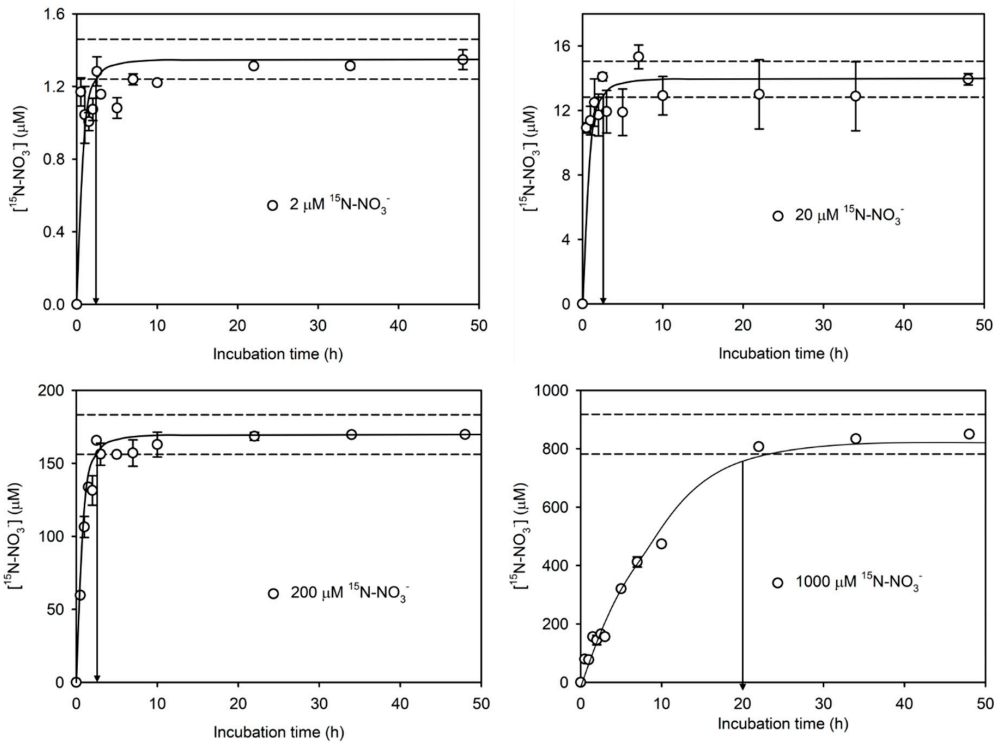

Figure 3. Results of the time series experiment targeting the proper incubation time to recover >95% of the added $^{15}N\text{-}NO_3^-$ converted into $^{30}N_2$. The plateau of $^{30}N_2$ production ±5%, shown graphically by the dotted lines, was defined experimentally from the slurries sacrificed after 48 h. Arrows indicate a minimum incubation time that in three out of four levels of nitrate is <5 h, while for the highest level is nearly 20 h. Continuous lines show graphically the temporal evolution of $^{15}N\text{-}NO_3^-$ recovery (= $^{30}N_2$ production). Each slurry was run in triplicate; averages and standard errors are reported.

3.3. Concentration Series Experiment

We tested the denitrification capacity of the riverine sediments we employed and the recovery of the added $^{15}N\text{-}NO_3^-$ with a concentration series experiment (Figure 4). With the slurry concentration of 167 mL L^{-1}, we obtained a rather good recovery of the added $^{15}N\text{-}NO_3^-$, averaging 86% over a wide range of labelled nitrate levels (from 0.5 to 800 μM). Thereafter, the enzymatic capacity of the denitrifier population in the sediment was saturated and the production of labelled N_2 became independent from the $^{15}N\text{-}NO_3^-$ concentration. The linear regression reported represents the calibration curve of this method, under the specific experimental settings described in Table 1. The calibration allows for converting the measured labelled dinitrogen into the original $^{15}N\text{-}NO_3^-$ concentration in the

water samples. Results from this test support the use of this assay over a wide range of $^{15}N\text{-}NO_3^-$ concentrations. It is however important to remark that each sediment needs to be tested in advance, and a similar calibration should be always performed together with the processing of samples from experiments with unknown $^{15}N\text{-}NO_3^-$ concentrations.

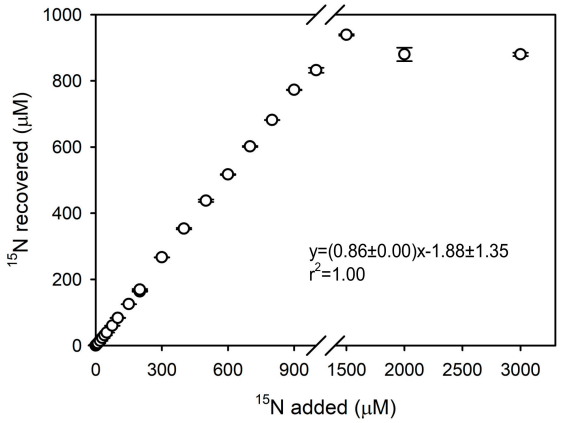

Figure 4. Recovered versus added $^{15}N\text{-}NO_3^-$ in a concentration series experiment. In addition, 24 standard solutions with increasing concentrations of $^{15}N\text{-}NO_3^-$ (from 0 to 3000 μM $^{15}N\text{-}NO_3^-$) were added to the sediment slurries and the produced labelled dinitrogen was quantified. The linear regression was calculated over the 0–800 μM $^{15}N\text{-}NO_3^-$ range. Each slurry was run in triplicate; averages and standard errors are reported.

3.4. Quantification of Labelled and Unlabeled N-NO_3^-

Standard solutions containing a wide range of combinations of labelled and unlabeled $N\text{-}NO_3^-$ underwent reduction in order to quantify the recovery of ^{15}N and ^{14}N. Due to the large background concentration of $^{28}N_2$, the ^{14}N is calculated from the measured $^{29}N_2$ and $^{30}N_2$ and not readily measured [5]. This may lead to large errors when the atom% of the ^{15}N in the total $N\text{-}NO_3^-$ pool is very low and the produced $^{29}N_2$ and $^{30}N_2$ deviate from the predictions of the binomial distribution. In the range between 16.5 to 83.5 atom% of ^{15}N, we recovered the same amount of ^{15}N atom% in the N_2 pool (Figure 5a). Outside this range, calculations produced large errors in the estimate of ^{14}N from the measured $^{29}N_2$ and $^{30}N_2$. This suggests, and confirms, that the enrichment of the $^{14}N\text{-}NO_3^-$ pool with labelled nitrate should be >15% to obtain precise measurements and calculations of ^{15}N and ^{14}N.

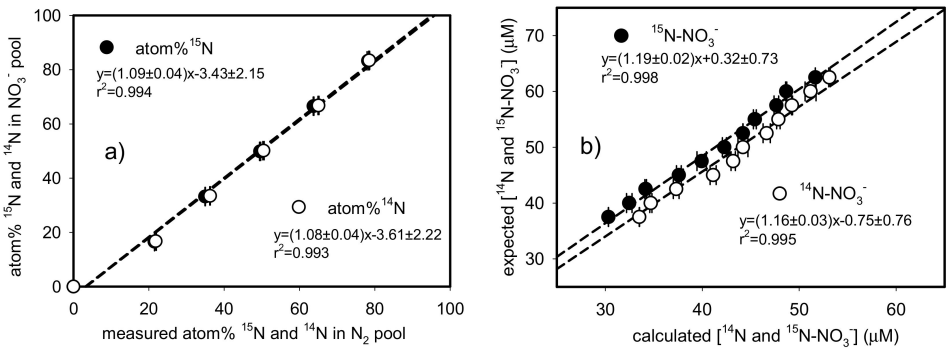

(**a**) (**b**)

Figure 5. ^{15}N atom% in the pool of N_2 produced by denitrification of different standard solutions containing mixtures of $^{14}N\text{-}NO_3^-$ and $^{15}N\text{-}NO_3^-$ versus ^{15}N atom% of the nitrate in the standards (**a**). Calculated versus added $^{14}N\text{-}NO_3^-$ and $^{15}N\text{-}NO_3^-$ concentrations in standard solutions containing mixtures of $^{14}N\text{-}NO_3^-$ and $^{15}N\text{-}NO_3^-$ (**b**). Details on concentrations of the two isotopes, incubation time, and slurry concentrations are reported in Table 1. Each slurry was run in triplicate; averages and standard errors are reported.

We performed a second validation of this method using standard solutions containing slightly different concentrations of $^{14}N\text{-}NO_3^-$ and $^{15}N\text{-}NO_3^-$, in order to see the accuracy of the method (Table 1 and Figure 5b). This second experiment confirmed the previous one and produced a very good fit between the recovered and expected concentrations of the labelled and unlabeled nitrate forms.

3.5. Anammox Assay

The ratio between the theoretical and measured $^{29}N_2$ concentrations along a $^{15}N\text{-}NO_3^-$ concentration series (from 5 to 200 µM) was 1, and it was independent of the labelled nitrate concentration, suggesting that anammox was not contributing to N_2 production in our anoxic slurries (Figure 6) [16]. The theoretical $^{29}N_2$ concentration was predicted by the binomial distribution of the $^{28/29/30}N_2$ accumulated during the incubation, assuming that bacterial denitrification was the only N_2 producing process. It is not surprising that anammox is not a relevant process in organic freshwater sediments [20,23,24], but this test should always be performed in order to verify the assumptions of [5] and avoid incorrect estimations of $^{28}N_2$ [16].

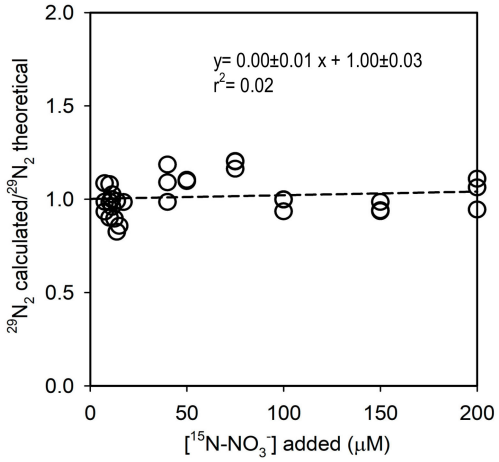

Figure 6. Ratios of calculated versus predicted $^{29}N_2$ along a concentration series of $^{15}N\text{-}NO_3^-$, targeting the co-occurrence of anammox and denitrification.

3.6. Measurements of $^{15}N\text{-}NO_3^-$ and $^{14}N\text{-}NO_3^-$ to Determine Nitrification Rates in Bioturbated Sediments

3.6.1. $^{14}N\text{-}NO_3^-$-Efflux from Sediments

In both treatments C and H, the application of $^{15}N\text{-}NO_3^-$ dilution allowed for calculating a net $^{14}N\text{-}NO_3^-$-efflux, significantly lower, by nearly 30%, in the presence of the oligochaetes (two way ANOVA, $p < 0.05$, Figure 7a). Results from calculations based on time series measurement of $^{14}N\text{-}NO_3^-$ and $^{15}N\text{-}NO_3^-$ (method A) tended to be lower than those based on method B [17] but differences were not significant (two way ANOVA, $p > 0.05$). Calculations with method B produced very comparable results if the term considering the natural abundance of $^{15}N\text{-}NH_4^+$ (0.366) was excluded from Equation (7) (method B *).

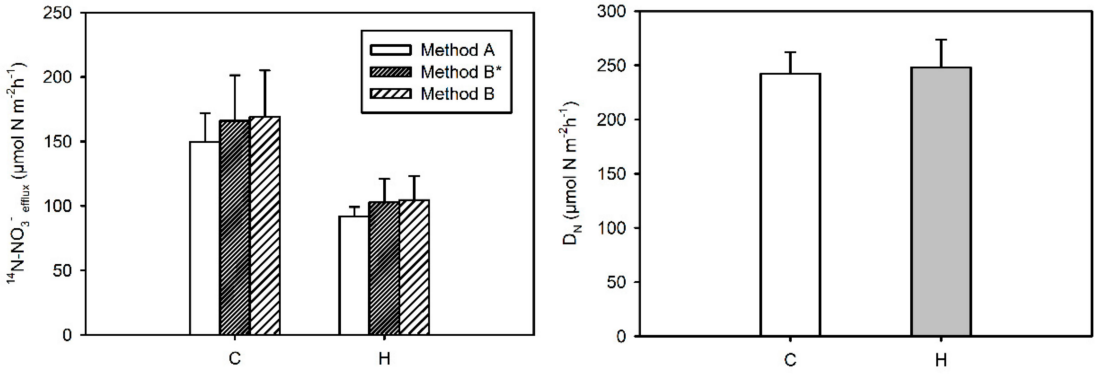

Figure 7. $^{14}N\text{-}NO_3^-$-efflux (**a**) and rates of denitrification of $^{14}N\text{-}NO_3^-$ produced within sediments via nitrification (D_N, **b**) measured in intact cores incubated in the dark. Method B * refers to calculations reported in [17] (Equation (7)) excluding the natural abundance of ^{15}N in the sedimentary ammonium pool. The group C ($n = 4$) had riverine sieved sediments whilst the group H ($n = 4$) had sieved sediments added with the oligochaete *S. tamesis* (800 ind m^{-2}).

3.6.2. Coupled Nitrification–Denitrification

Denitrification rates of the $^{14}N\text{-}NO_3^-$ produced within sediments via nitrification (D_N, Figure 7b) were not statistically different in bare and bioturbated sediments (t-test, $p > 0.05$), and averaged 245 ± 30 µmol N m^{-2} h^{-1}. Rates of denitrification of water column $^{14}N\text{-}NO_3^-$, not reported, were 102 ± 23 and 119 ± 10 µmol N m^{-2} h^{-1} in C and H, respectively. They tended to be higher in the presence of *S. tamesis* but differences were not significant (t test, $p > 0.05$).

Overall, calculated nitrification rates ($^{14}N\text{-}NO_3^-$-efflux + D_N) in the riverine sediments used in our experiment were among the highest reported in the literature, averaging 408 ± 40 and 350 ± 31 µmol N m^{-2} h^{-1} in C and H, respectively [25–27]. It is surprising, but not entirely novel, that a deep burrower as *S. tamesis* is not enhancing but depressing rates of nitrification, and it is not stimulating the rates of denitrification. Similar results are reported for another opportunistic polychaete that has invaded the Baltic Sea (*Marenzelleria* spp.) and is able to cope with anoxic and chemically reduced conditions in the pore water. *Marenzelleria* was demonstrated to stimulate more the dissimilative reduction of nitrate to ammonium (DNRA) than denitrification, likely due to the occurrence of free sulphides in its burrow, which are toxic to denitrifiers [28]. We speculate that *S. tamesis* adds to the list of pioneer species able to colonize very organic sediments, not requiring frequent ventilation of their burrows or acting as conveyors (sensu [29]). These bioturbators in fact ventilate their burrows extracting anoxic pore water from surrounding sediments, without creating significant toxic niches and without any stimulation of nitrifiers growth.

4. Conclusions

The proposed approach represents a relatively easy method to quantify accurately dissolved $N\text{-}NO_3^-$ in mixtures of $^{14}N\text{-}NO_3^-$ and $^{15}N\text{-}NO_3^-$ in freshwater. Instead of using pure cultures of denitrifiers, that may require specific skills, or different chemicals to reduce the nitrate pool, we used natural populations of denitrifiers from the sampling site where we performed the nitrification experiment, after calibration of their performances. As we used organic sediments from a nitrate-rich river, our slurry displayed a very large denitrification potential, being able to reduce quantitatively standards up to 800 µM $^{15}N\text{-}NO_3^-$, but no measurable anammox. The recovery of $^{14}N\text{-}NO_3^-$ and $^{15}N\text{-}NO_3^-$ from standards with different ratios of the two isotopes was also satisfactory, along a wide range of ^{15}N atom%. It is important to always check for the concurrence of anammox, which would result in the violation of the assumptions related to the binomial distribution of $^{28/29/30}N_2$ [5]. Our specific test demonstrated that, in the Mincio River sediments, the production of $^{29}N_2$ was

unaffected by increasing concentrations of $^{15}N\text{-}NO_3^-$, suggesting a negligible role of anammox bacteria in N_2 production. However, in the case of adopting the present approach, the sediments and their performances need to be specifically tested. The accurate measurement of $^{14}N\text{-}NO_3^-$ and $^{15}N\text{-}NO_3^-$ concentrations has different applications in ecological studies of microbial N transformations. One of these is the quantification of ammonium oxidation to nitrate in bioturbated sediments, via the $^{15}N\text{-}NO_3^-$ dilution technique. Nitrification rates in intact sediments are generally modelled and seldom experimentally measured as compared to processes such as denitrification or nitrate ammonification. However, in oligotrophic aquatic ecosystems, nitrification is the only source of nitrate for the above-mentioned processes. The application of our slurry approach to nitrification measurements in bioturbated sediments allowed to demonstrate that not all burrowers, as generally reported in the literature, provide ecosystem services such as the increase of the toxic sediment volume and the stimulation of N loss via coupled nitrification–denitrification.

Author Contributions: Conceptualization, P.C.M., S.B., and M.B.; validation, P.C.M., D.M.A.G., and F.V.; formal analysis, F.V. and S.B.; resources, M.B. and G.C.; writing—original draft preparation, P.C.M., S.B., and M.B.; writing—review and editing, D.M.A.G, G.C, and E.A.F.

Funding: This research received no external funding.

Acknowledgments: Paula Carpintero Moraes was supported by Conselho Nacional de Desenvolvimento Científico e Tecnológico (CNPq-Brasil); Marco Bartoli was supported by the INBALANCE (Invertebrate-BacteriAL Associations as hotspots of benthic Nitrogen Cycling in Estuarine ecosystems) project, funded by the European Social Fund according to the activity 'Improvement of researchers' qualification by implementing world-class R&D projects' of Measure No. 09.3.3-LMT-K-712-01-0069).

Conflicts of Interest: The authors declare no conflict of interest.

References

1. Galloway, J.N.; Dentener, F.J.; Capone, D.G.; Boyer, E.W.; Howarth, R.W.; Seitzinger, S.P.; Asner, G.P.; Cleveland, C.C.; Green, P.A.; Holland, E.A.; et al. Nitrogen cycles: Past, present, and future. *Biogeochemistry* **2004**, *70*, 153–226. [CrossRef]
2. Risgaard-Petersen, N.; Nielsen, L.P.; Blackburn, T.H. Simultaneous measurement of benthic denitrification, with the isotope pairing technique and the N_2 flux method in a continuous flow-through system. *Water Res.* **1998**, *32*, 3371–3377. [CrossRef]
3. Marchant, H.K.; Lavik, G.; Holtappels, M.; Kuypers, M.M.M. The fate of nitrate in intertidal permeable sediments. *PLoS ONE* **2014**, *9*, e104517. [CrossRef]
4. Newell, S.E.; McCarthy, M.J.; Gardner, W.S.; Fulweiler, R.W. Sediment nitrogen fixation: A call for re-evaluating coastal N budgets. *Estuaries Coasts* **2016**, *39*, 1626–1638. [CrossRef]
5. Nielsen, L.P. Denitrification in sediment determined from nitrogen isotope pairing. *FEMS Microbiol. Ecol.* **1992**, *86*, 357–362. [CrossRef]
6. Burgin, A.J.; Hamilton, S.K. Have we overemphasized the role of denitrification in aquatic ecosystems? A review of nitrate removal pathways. *Front. Ecol. Environ.* **2007**, *5*, 89–96. [CrossRef]
7. Risgaard-Petersen, N.; Rysgaard, S.; Revsbech, N.P. A sensitive assay for determination of $^{14}N/^{15}N$ isotope distribution in NO_3^-. *J. Microbiol. Methods* **1993**, *17*, 155–164. [CrossRef]
8. Jensen, K.M.; Jensen, M.H.; Cox, R.P. Membrane inlet mass spectrometric analysis of N-isotope labelling for aquatic denitrification studies. *FEMS Microbiol. Ecol.* **1996**, *20*, 101–109. [CrossRef]
9. An, S.; Gardner, W.S.; Kana, T. Simultaneous measurement of denitrification and nitrogen fixation using isotope pairing with membrane inlet mass spectrometry analysis. *Appl. Environ. Microbiol.* **2001**, *67*, 1171–1178. [CrossRef]
10. Bonaglia, S.; Deutsch, B.; Bartoli, M.; Marchant, H.K.; Brüchert, V. Seasonal oxygen, nitrogen and phosphorus benthic cycling along an impacted Baltic Sea estuary: Regulation and spatial patterns. *Biogeochemistry* **2014**, *119*, 139–160. [CrossRef]
11. Kana, T.M.; Darkangelo, C.; Oldham, J.B.; Bennett, G.E.; Cornwell, J.C. Membrane inlet mass spectrometer for rapid high-precision determination of N_2, O_2, and Ar in environmental water samples. *Anal. Chem.* **1994**, *66*, 4166–4170. [CrossRef]

12. Heiss, E.M.; Fulweiler, R.W. Coastal water column ammonium and nitrite oxidation are decoupled in summer. *Estuar. Coast. Shelf Sci.* **2016**, *178*, 110–119. [CrossRef]
13. Revesz, K.; Böhlke, J.K.; Yoshinari, T. Determination of ^{18}O and ^{15}N in nitrate. *Anal. Chem.* **1997**, *69*, 4375–4380. [CrossRef] [PubMed]
14. McIlvin, M.R.; Altabet, M.A. Chemical conversion of nitrate and nitrite to nitrous oxide for nitrogen and oxygen isotopic analysis in freshwater and seawater. *Anal. Chem.* **2005**, *77*, 5589–5595. [CrossRef]
15. Soana, E.; Naldi, M.; Bonaglia, S.; Racchetti, E.; Castaldelli, G.; Brüchert, V.; Viaroli, P.; Bartoli, M. Benthic nitrogen metabolism in a macrophyte meadow (*Vallisneria spiralis* L.) under increasing sedimentary organic matter loads. *Biogeochemistry* **2015**, *124*, 387–404. [CrossRef]
16. Risgaard-Petersen, N.; Nielsen, L.P.; Rysgaard, S.; Dalsgaard, T.; Meyer, R.L. Application of the isotope pairing technique in sediments where anammox and denitrification coexist. *Limnol. Oceanogr. Methods* **2003**, *1*, 63–73. [CrossRef]
17. Rysgaard, S.; Risgaard-Petersen, N.; Nielsen, L.P.; Revsbech, N.P. Nitrification and denitrification in lake and estuarine sediments measured by the ^{15}N dilution technique and isotope pairing. *Appl. Environ. Microbiol.* **1993**, *59*, 2093–2098.
18. Ribaudo, C.; Bartoli, M.; Racchetti, E.; Longhi, D.; Viaroli, P. Seasonal fluxes of O_2, DIC and CH_4 in sediments with *Vallisneria spiralis*: Indications for radial oxygen loss. *Aquat. Bot.* **2001**, *94*, 134–142. [CrossRef]
19. Rota, E.; Bartoli, M.; Laini, A. First time in Italy. Is the elusive aquatic megadrile Sparganophilus Benham, 1892 (Annelida, Clitellata) accelerating its dispersal in Europe? *J. Limnol.* **2014**, *73*, 482–489. [CrossRef]
20. Ruginis, T.; Bartoli, M.; Petkuviene, J.; Zilius, M.; Lubiene, I.; Laini, A.; Razinkovas-Baziukas, A. Benthic respiration and stoichiometry of regenerated nutrients in lake sediments with Dreissena polymorpha. *Aquat. Sci.* **2014**, *76*, 405–417. [CrossRef]
21. Zhou, S.; Borjigin, S.; Riya, S.; Terada, A.; Hosomi, M. The relationship between anammox and denitrification in the sediment of an inland river. *Sci. Total Environ.* **2014**, *490*, 1029–1036. [CrossRef] [PubMed]
22. Racchetti, E.; Bartoli, M.; Soana, E.; Longhi, D.; Christian, R.R.; Pinardi, M.; Viaroli, P. Influence of hydrological connectivity of riverine wetlands on nitrogen removal via denitrification. *Biogeochemistry* **2011**, *103*, 335–354. [CrossRef]
23. Wang, S.; Zhu, G.; Peng, Y.; Jetten, M.S.M.; Yin, C. Anammox bacterial abundance, activity, and contribution in riparian sediments of the Pearl River estuary. *Environ. Sci. Technol.* **2012**, *46*, 8834–8842. [CrossRef] [PubMed]
24. Zhao, Y.; Xia, Y.; Kana, T.M.; Wu, Y.; Li, X.; Yan, X. Seasonal variation and controlling factors of anaerobic ammonium oxidation in freshwater river sediments in the Taihu Lake region of China. *Chemosphere* **2013**, *93*, 2124–2131. [CrossRef]
25. Pauer, J.J.; Aue, M.T. Nitrification in the water column and sediment of a hypereutrophic lake and adjoining river system. *Water Res.* **2000**, *34*, 1247–1254. [CrossRef]
26. Svensson, J.M.; Enrich-Prast, A.; Leonardson, L. Nitrification and denitrification in a eutrophic lake sediment bioturbated by oligochaetes. *Aquat. Microb. Ecol.* **2001**, *23*, 177–186. [CrossRef]
27. Strauss, E.A.; Lamberti, G.A. Effect of dissolved organic carbon quality on microbial decomposition and nitrification rates in stream sediments. *Freshw. Biol.* **2002**, *47*, 65–74. [CrossRef]
28. Bonaglia, S.; Bartoli, M.; Gunnarsson, J.S.; Rahm, L.; Raymond, C.; Svensson, O.; Shakeri Yekta, S.; Brüchert, V. Effect of reoxygenation and Marenzelleria spp. bioturbation on Baltic Sea sediment metabolism. *Mar. Ecol. Prog. Ser.* **2013**, *482*, 43–55. [CrossRef]
29. Kristensen, E.; Penha-Lopes, G.; Delefosse, M.; Valdemarsen, T.; Quintana, C.O.; Banta, G.T. What is bioturbation? The need for a precise definition for fauna in aquatic sciences. *Mar. Ecol. Prog. Ser.* **2012**, *446*, 285–302. [CrossRef]